TÜBİTAK

Turkish Journal of Chemistry

http://journals.tubitak.gov.tr/chem/

Research Article

Turk J Chem
(2019) 43: 1646 – 1655
© TÜBİTAK
doi:10.3906/kim-1909-32

Synthesis, characterization, and investigation of singlet oxygen, DNA interaction, and topoisomerase I inhibition properties of novel zinc(II) phthalocyanine

Ümit DEMİRBAŞ*
Department of Chemistry, Faculty of Science, Karadeniz Technical University, Trabzon, Turkey

Received: 11.09.2019 • **Accepted/Published Online:** 04.11.2019 • **Final Version:** 09.12.2019

Abstract: In this work, phthalonitrile (**3**) and zinc(II) phthalocyanine (**4**) were prepared. To determine the photodynamic therapy potential of compound **4**, singlet oxygen quantum yield, DNA binding and cleavage, and topoisomerase I inhibition experiments were performed. The singlet oxygen quantum yield value of compound **4** was found higher than that of the standard unsubstituted zinc(II) phthalocyanine compound (Std-ZnPc). The binding experiments showed that compound **4** interacted with ct-DNA strongly via nonintercalation mode. pBR322 plasmid DNA cleavage activity of the compound was investigated using agarose gel electrophoresis. The results showed that the compound **4** had important DNA cleavage activity. The *E. coli* DNA topoisomerase I inhibition effects of compound **4** were investigated using agarose gel electrophoresis. Compound **4** had an *E. coli* topoisomerase I inhibitory effect at increasing concentrations. The results showed that compound **4** has photosensitizer potential in photodynamic therapy.

Key words: DNA-binding, topoisomerase I, DNA-photocleavage, phthalocyanine

1. Introduction

Cancer is a common fatal disease caused by uncontrolled cell division [1,2]. The prevention of this division is the most important stage for cancer treatment. The common side effects of conventional treatment methods inspired scientists to find new cancer treatment methods [3,4]. Photodynamic therapy (PDT) is a new and alternative cancer treatment method. PDT is based on the production of singlet oxygen by a photosensitizer compound under light irradiation and the resulting singlet oxygen breaks down cancerous tissues [5,6]. PDT has advantages such as being noninvasive, having low side effects and high selectivity to tissues, and possessing the ability to be combined with other treatments. These advantages make PDT superior to other cancer treatment methods [7,8].

Phthalocyanines (Pcs) are aromatic macrocyclic compounds formed by isoindole units. Thanks to their strong π conjugation, high chemical stabilities, and optical properties they are used in many different applications [9–15]. Photodynamic therapy (PDT) is a new cancer treatment method. It takes place with the irradiation of the photosensitizer compound by light in the presence of oxygen. The singlet oxygen formed during the irradiation breaks down the cancerous tissues. [16]. Therefore, the singlet oxygen quantum yield is very important for a photosensitizer compound. Their visible region absorptions, low toxicity in the dark, and high singlet oxygen yields allow phthalocyanines to be used in PDT [17].

Topoisomerase I is an enzyme that dissolves DNA supercoiling during replication and transcription [18,19].

*Correspondence: udemirbas@ktu.edu.tr

This work is licensed under a Creative Commons Attribution 4.0 International License.

The level of topoisomerase I in cancerous cell is much higher than in normal cells [20,21]. The inhibition of topoisomerase I is one of the important points of cancer treatment because it can cause DNA damage and stop DNA replication [22]. To stop the proliferation of cancerous cells by preventing uncontrolled cell division, the inhibition of topoisomerase I is a useful treatment method [23].

DNA binding experiments are very important to understand the interaction of compounds with DNA. The interaction of compounds with DNA gives important information about their potential to be used in anticancer applications. DNA photocleavage experiments are important for determination of the anticancer potential of a compound with the breakdown of the DNA of the cancerous cells [24,25].

In this study, it was planned to synthesize peripherally tetra 4-(1-phenoxypropan-2-yloxy)-substituted novel zinc(II) phthalocyanine and investigate its photosensitizer potential in photodynamic therapy. To determine this potential, singlet oxygen quantum yield experiments, DNA binding studies (to investigate the interaction with DNA), DNA cleavage studies (to investigate the photonuclease activity), and topoisomerase I inhibition properties of the novel zinc(II) phthalocyanine were determined.

2. Experimental

All information about the used equipment, materials, synthesis, singlet oxygen, DNA binding, DNA photocleavage, *E. coli* topoisomerase formulas, and parameters is given in the Supplementary information.

3. Results and discussion

3.1. Synthesis and characterization

The synthetic pathway of the novel compounds is shown in Figure 1. The phthalonitrile compound 4-(1-phenoxypropan-2-yloxy)phthalonitrile (**3**) was prepared with a reaction between 1-phenoxy-2-propanol (**1**) and 4-nitrophthalonitrile (**2**) in DMF in the presence of K_2CO_3. The novel phthalonitrile compound (**3**) was characterized by a combination of ^{1}H and ^{13}C NMR, FT-IR, and mass spectral data. In the IR spectrum, new vibrations monitored at 2229 cm^{-1} demonstrated that compound **3** has nitrile groups. In the ^{1}H NMR spectrum of compound **3**, aromatic and aliphatic protons showed the expected signals. In the ^{13}C NMR spectrum**,** the nitrile carbon signals at 115.698 and 115.276 ppm indicated that substitution was achieved. In the mass spectra the $[M+H]^+$ peak confirmed the proposed structure of compound **3**.

Zinc(II) phthalocyanine **4** was prepared with a reaction between starting compound **3** and zinc acetate in n-pentanol. Novel phthalocyanine **4** was characterized by a combination of ^{1}H NMR, FT-IR, UV-Vis, and mass spectral data. The evanescence of -C≡N vibrations in the IR spectrum of compound **4** confirmed completion of the cyclotetramerization reaction. In the ^{1}H NMR spectrum of compound **4** aromatic and aliphatic protons showed the expected signals. In the mass spectrum of compound **4** the observed $[M+H]^+$ peak confirmed the proposed structure. In the UV-Vis spectrum, the Q band of compound **4** was monitored at 679 nm and the B band was monitored at 353 nm. All characterization data are in accordance with the literature about the metallophthalocyanines [26,27].

3.2. Singlet oxygen quantum yields

For the PDT performance of a photosensitizer, singlet oxygen generation is very important. An energy transfer takes place between the triplet state of a photosensitizer and the ground state molecular oxygen when the photosensitizer is irradiated by light and singlet oxygen is produced. Therefore, the singlet oxygen quantum

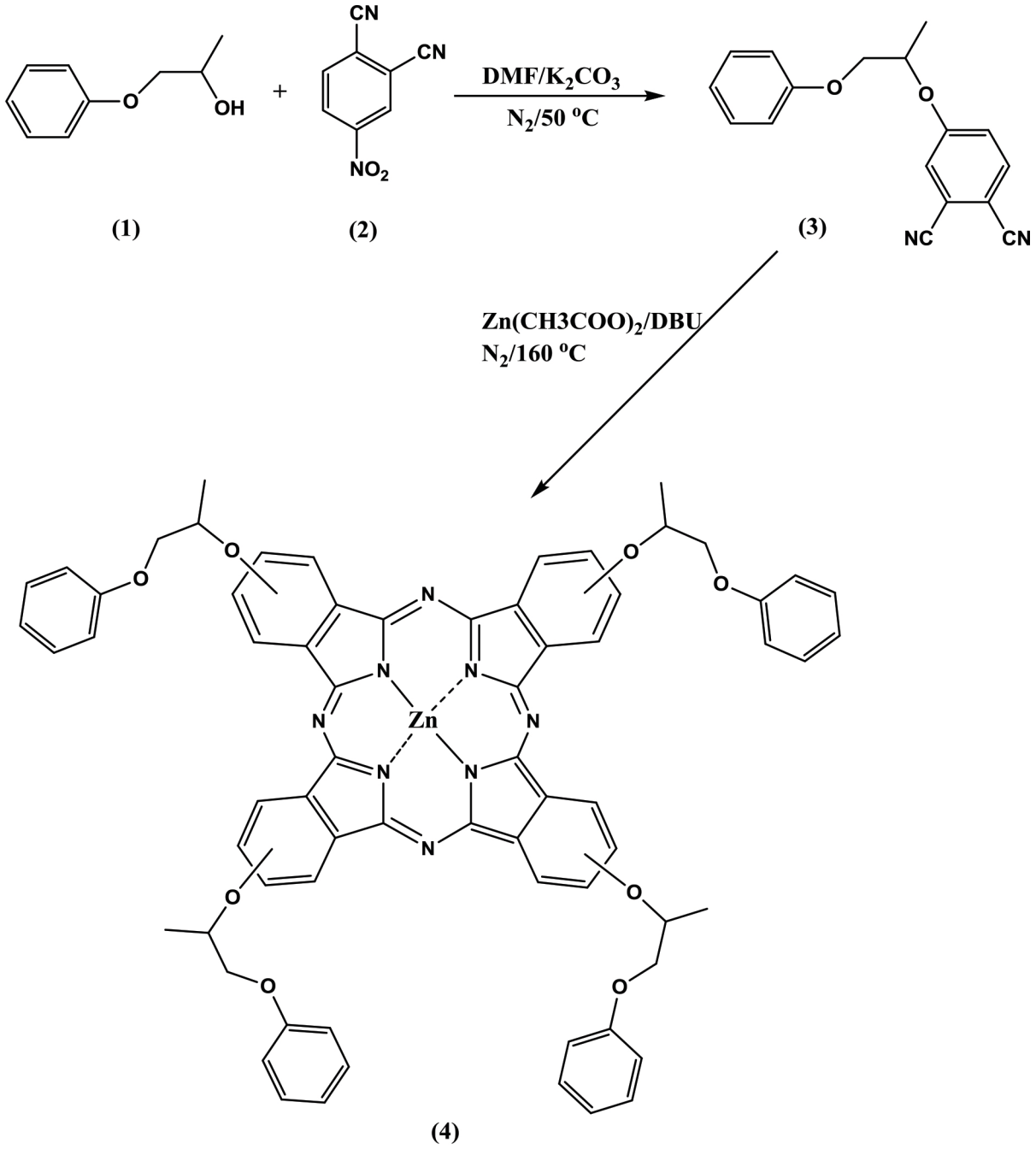

Figure 1. Synthetic route of novel compounds **3** and **4**.

yield value is the most important parameter to determine the potential of compounds as photosensitizers in PDT for cancer. The singlet oxygen quantum yield (Φ_Δ) value of compound **4** was determined in DMSO by using 1,3-diphenylisobenzofuran (DPBF) as a singlet oxygen quencher. DPBF absorbance at 417 nm decreased due to the singlet oxygen generation. The Q band intensity of compound **4** did not change (Figure 2) and this showed that compound **4** did not undergo any decomposition during the experiment. The Φ_Δ value of compound **4** (0.71) was found to be higher than that of the standard zinc(II) phthalocyanine (0.67). This showed that

the substitution of 4-(1-phenoxypropan-2-yloxy) groups on the phthalocyanine ring make compound **4** more effective than standard Znpc for PDT applications. The experimental results showed that compound **4** has higher singlet oxygen quantum yield than the zinc(II) phthalocyanine derivatives in literature [28,29].

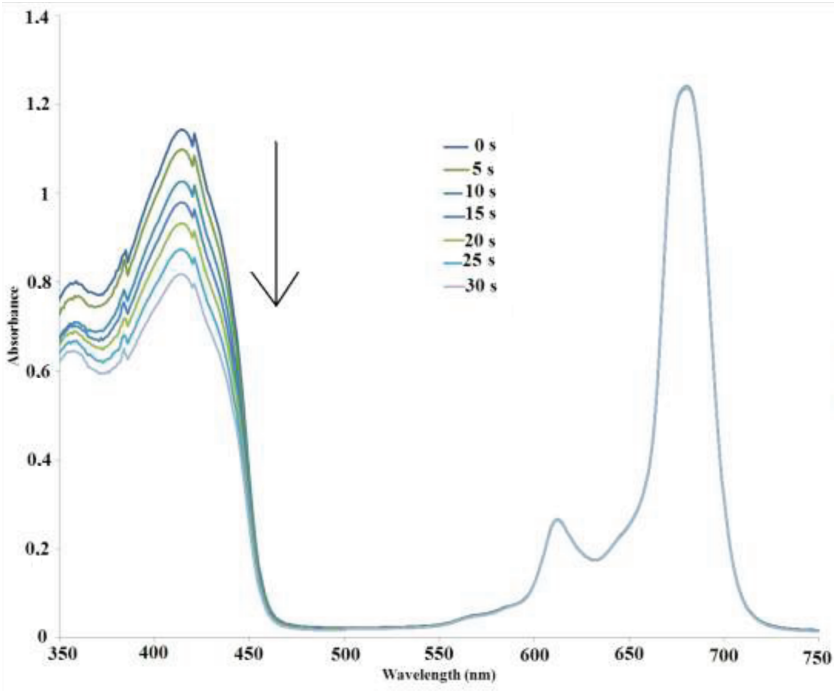

Figure 2. The determination of the singlet oxygen quantum yield of compound **4** in DMSO at 1×10^{-5} M (inset: plots of DPBF absorbance versus time).

3.3. DNA binding studies

UV-Vis absorption experiments allow the determination of the DNA binding ability of complexes. When compounds interact with ct-DNA in intercalation mode, hypochromic and bathochromic effects are observed. On the other hand, the binding of metal complexes to ct-DNA via nonintercalative mode causes hyperchromic or low hypochromic effects. In this work, the DNA interaction mode of compound **4** was investigated as described in previous studies [30,31]. The results of DNA binding studies are given in the Table. As shown in Figure 3, the maximum absorbance of compound **4** was at 681 nm. The UV-Vis spectrum of the compound demonstrated a hypochromic effect (27.97%) after the addition of ct-DNA. According to the Wolfe–Shimmer equation (Eq. 3), the binding constant (K_b) of compound **4** was calculated as $1.73 \pm 0.50 \times 10^4\ \mathrm{M}^{-1}$.

Table 1. ct-DNA binding data of compound **4**.

Compound	λ (nm)	Change in Abs.	Shift (nm)	$K_b(\mathrm{M}^{-1})$	H%
Compound **4**	681	Hypochromism	0	$1.73 \pm 0.50 \times 10^4$	27.97

To confirm the interaction mode between compound **4** and ct-DNA, an EB competitive binding study was performed as described previously [32,33]. The EB-(ct-DNA) complex was formed by adding EB:ct-DNA (75 μM : 75 μM) solution and gradually varying the concentrations of compound **4**, measured as the changes

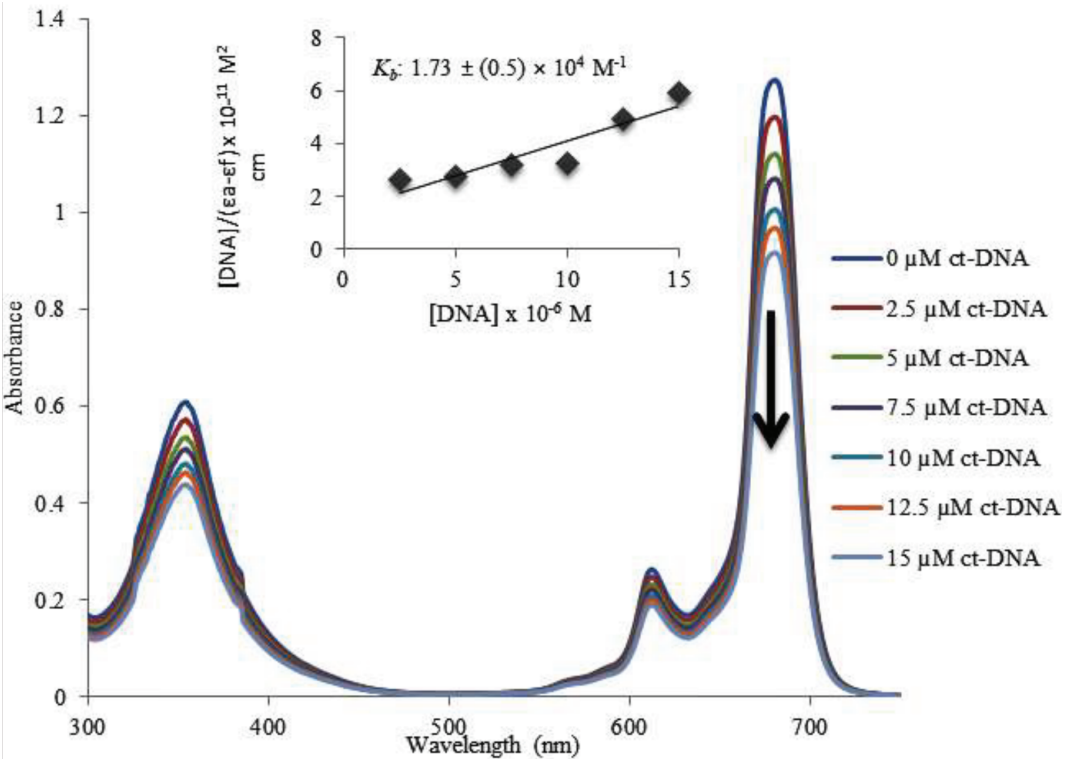

Figure 3. Absorption spectrum of compound **4** in the absence and presence of increasing amounts of ct-DNA.

in the absorption spectra in the range of 425–550 nm. The result is shown in Figure 4. The UV spectrum of the EB competitive binding study was measured in the range of 550–425 nm and maximum absorbance was at 481 nm. After addition of ct-DNA, absorbance decreased and a red shift was observed. This result showed that EB interacted with ct-DNA via intercalation and formed the EB-(ct-DNA) complex. The absorbance did not change upon addition of varying concentrations of compound. This suggested that compound **4** interacts with ct-DNA via nonintercalation mode.

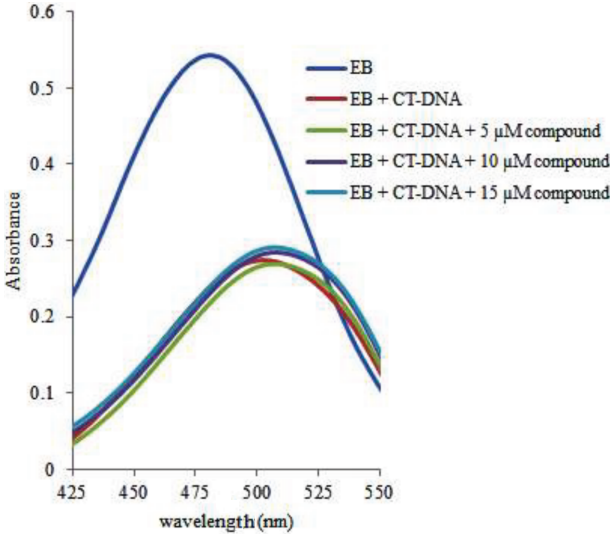

Figure 4. Absorption spectra of free EB and EB bound to ct-DNA in the absence and presence of increasing amounts of compound **4**.

3.4. pBR322 plasmid DNA cleavage activities

pBR322 plasmid DNA cleavage properties of compound **4** were investigated using agarose gel electrophoresis without/with irradiation. The DNA photocleavage experiments were carried out with white light irradiation (17.5 mW cm^{-2}, 10 min). When one-strand cleavage of supercoiled plasmid DNA (Sc) generates the nicked form (Nc), two-strand cleavage of Sc occurs in linear form (Ln) that moves between Sc and Nc [34,35]. The results of cleavage properties of compound **4 a**re shown in Figures 5 and 6. As shown in Figure 5, no concentrations of compound **4** showed any cleavage effect. On the other hand, Figure 6 shows that Nc increased in the presence of the compound at 12.5, 25, and 50 μM. This result reveals that compound **4** showed DNA cleavage activities due to its singlet oxygen quantum yield. In addition, H_2O_2 was used as an oxidative activator to begin the DNA cleavage process. The results of oxidative cleavage experiments are presented in Figures 7 and 8. These results showed that the presence of H_2O_2 did not affect the DNA cleavage effects of compound **4** in the dark but the DNA photocleavage of the compound was significantly increased with light irradiation in the presence of H_2O_2 because the band intensity of Nc and Ln increased.

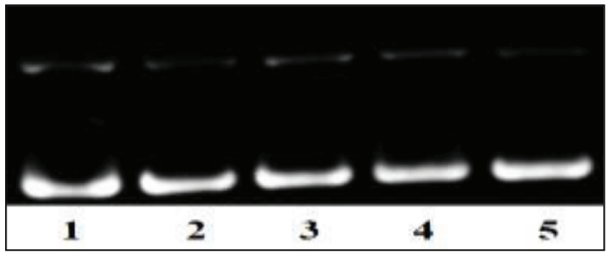

Figure 5. Agarose gel electrophoresis of pBR322 plasmid DNA in the absence and presence of compound **4** without irradiation. Lane 1: DNA control; lanes 2–5: DNA + compound **4** (6.25, 12.5, 25, and 50 μM).

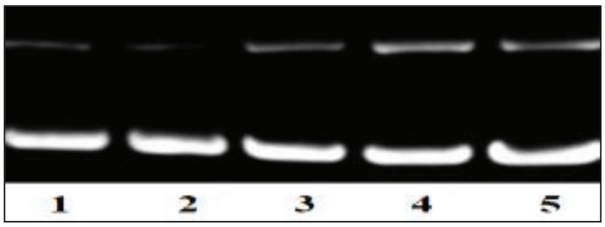

Figure 6. Agarose gel electrophoresis of pBR322 plasmid DNA in the absence and presence of compound **4** with white light irradiation. Lane 1: DNA control; lanes 2–5: DNA + compound **4** (6.25, 12.5, 25 and 50 μM).

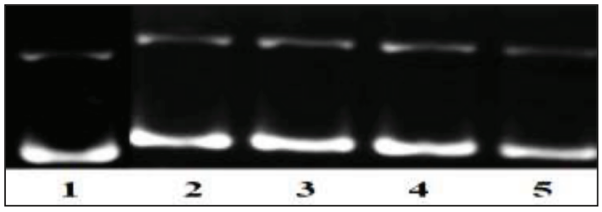

Figure 7. Oxidative pBR322 plasmid DNA cleavage in the presence of H_2O_2 without irradiation. Lane 1: DNA control; lanes 2–5: DNA + compound **4** (6.25, 12.5, 25, and 50 μM) + H_2O_2 (0.4 M).

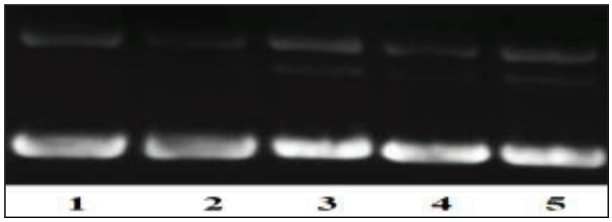

Figure 8. Oxidative pBR322 plasmid DNA cleavage in the presence of H_2O_2 with white light irradiation. Lane 1: DNA control; lanes 2–5: DNA + compound **4** (6.25, 12.5, 25, and 50 μM) + H_2O_2 (0.4 M) + 10 min irradiation.

3.5. *E.* coli topoisomerase I inhibition

The *E. coli* DNA topoisomerase I inhibition effect of compound **4** was investigated using agarose gel electrophoresis and the result was analyzed using a computer program. The results are shown in Figure 9. *E. coli* topoisomerase I (2 units) and pBR322 plasmid DNA were mixed and incubated at 37 °C for 1 h as a negative control as shown in Figure 9, lane 2. This result showed that Sc converted to Nc (7.60%) and Ln (59.10%). Compound **4** had low *E. coli* topoisomerase I inhibitory effects at increasing concentrations (Figure

9, lanes 3–5). At 12.5, 25, and 50 μM, the band intensity of Ln was calculated as 56.00%, 53.50%, and 46.20%, respectively.

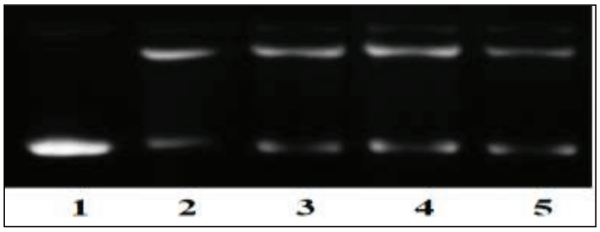

Figure 9. The inhibitory properties of *E. coli* topoisomerase I. Lane 1: DNA control; lane 2: DNA + 2 units of topoisomerase; lanes 3–5: DNA + 2 units of topoisomerase + compound **4** (12.5, 25 and 50 μM).

3.6. Conclusions

Phthalonitrile compound **3** was prepared with a reaction between 1-phenoxy-2-propanol (**1**) and 4-nitrophthalonitrile (**2**). Peripherally tetra-substituted zinc(II) phthalocyanine complex **4** was prepared with the cyclotetramerization reaction of compound **3** in n-pentanol. Novel compounds **3** and **4** were characterized by a combination of different spectroscopic techniques such as FT-IR, ^{1}H NMR, ^{13}C NMR, UV-Vis, and mass analysis. The singlet oxygen quantum yield (Φ_{Δ}) value of compound **4** was determined in DMSO by using 1,3-diphenylisobenzofuran (DPBF) as a singlet oxygen quencher. The Φ_{Δ} value of compound **4** (0.71) was found higher than that of standard zinc(II) phthalocyanine (0.67), suggesting the effect of the substitution of 4-(1-phenoxypropan-2-yloxy) groups on the phthalocyanine skeleton. UV-Vis absorption experiments were performed to determine the DNA binding ability of the compounds. UV-Vis absorption titration and EB competitive binding experiments showed that compound **4** interacted with ct-DNA strongly via nonintercalation mode. pBR322 plasmid DNA cleavage activities of the compound were investigated using agarose gel electrophoresis without/with irradiation. The results revealed that compound **4** showed DNA cleavage activities due to its singlet oxygen quantum yield. The *E. coli* DNA topoisomerase I inhibition effects of compound **4** were investigated using agarose gel electrophoresis and the results were analyzed using Image Lab Version 4.0.1. The compound had *E. coli* topoisomerase I inhibitory effects at increasing concentrations. The results showed that compound **4** can be used as a photosensitizer agent in photodynamic therapy.

References

1. Ferlay J, Soerjomatarm I, Dikshit R, Eser S, Mathers C et al. Cancer incidence and mortality worldwide: Sources, methods and major patterns in GLOBOCAN 2012. International Journal of Cancer 2015; 136 (5): 359-386. doi: 10.1002/ijc.29210
2. Uslan C, Sesalan BŞ. The synthesis, photochemical and biological properties of new silicon phthalocyanines. Inorganica Chimica Acta 2013; 394: 353-362. doi: 10.1016/j.ica.2012.08.004
3. Pradeepa SM, Bhojya Naik HS, Vinay Kumar B, Indira Priyadarsini K, Barik A et al. Synthesis and characterization of cobalt(II), nickel(II) and copper(II)-based potential photosensitizers: evaluation of their DNA binding profile, cleavage and photocytotoxicity. Inorganica Chimica Acta 2015; 428: 138-146.
4. Zheng BY, Shen XM, Zhao DM, Cai YB, Ke MR et al. Silicon(IV) phthalocyanines substituted axially with different nucleoside moieties. Effects of nucleoside type on the photosensitizing efficiencies and in vitro photodynamic activities. Journal of Photochemistry and Photobiology B-Biology 2016; 159: 196-204. doi: 10.1016/j.jphotobiol.2016.03.055

5. Kawczyk-Krupka A, Bugaj AM, Latos W, Zaremba K, Wawrzyniec K et al. Photodynamic therapy in colorectal cancer treatment–The state of the art in preclinical research, Photodiagnosis and Photodynamic Therapy 2016; 13: 158-174. doi: 10.1016/j.pdpdt.2015.07.175

6. Banerjee SM, MacRobert AJ, Mosse CA, Periera B, Bown SG et al. Photodynamic therapy: inception to application in breast cancer. Breast 2017; 31: 105-113. doi: 10.1016/j.breast.2016.09.016

7. Oniszczuk A, Wojtunik-Kulesza KA, Oniszczuk T, Kasprzak K. The potential of photodynamic therapy (PDT)-Experimental investigations and clinical use. Biomedicine & Pharmacotherapy 2016; 83: 912-929. doi: 10.1016/j.biopha.2016.07.058

8. Kwiatkowski S, Knap B, Przystupski D, Saczkoc J, Kedziersk E et al. Photodynamic therapy – mechanisms, photosensitizers and combinations. Biomedicine & Pharmacotherapy 2018; 106: 1098-1107. doi: 10.1016/j.biopha.2018.07.049

9. Leznoff CC, Lever ABP. Phthalocyanines Properties and Applications. Vol. 1. New York, NY, USA: VCH Publisher, 1989.

10. De La Torre G, Vazquez P, Agullo-Lopez F, Torres T. Phthalocyanines and related compounds: organic targets for nonlinear optical applications. Journal of Materials Chemistry 1998; 8: 1671-1683. doi: 10.1039/A803533D

11. Yang F, Forrest SR. Photocurrent generation in nanostructured organic solar cells. ACS Nano 2008; 2 (5): 1022-1032. doi: 10.1021/nn700447t

12. Leznoff CC, Lever ABP. Phthalocyanines Properties and Applications. Vol. 4. New York, NY, USA: VCH Publisher, 1996.

13. Zagal JH, Griveua S, Silva JF, Nyokong T, Bedioui F. Metallophthalocyanine-based molecular materials as catalysts for electrochemical reactions. Coordination Chemistry Reviews 2010; 254: 2755-2791. doi: 10.1016/j.ccr.2010.05.001

14. Ağırtaş MS, Cabir B, Özdemir S. Novel metal (II) phthalocyanines with 3, 4, 5-trimethoxybenzyloxy-substituents: synthesis, characterization, aggregation behaviour and antioxidant activity. Dyes Pigments 2013; 96: 152-157. doi: 10.1016/j.dyepig.2012.07.023

15. Oliveira LT, Garcia GM, Kano EK, Tedesco AC, Mosqueira VC. HPLC-FLD methods to quantify chloroaluminum phthalocyanine in nanoparticles, plasma and tissue: application in pharmacokinetic and biodistribution studies. Journal of Pharmaceutical and Biomedical Analysis 2011; 56: 70-77. doi: 10.1016/j.jpba.2011.04.016

16. Bayrak R, Akçay HT, Durmuş M, Değirmencioğlu İ. Synthesis, photophysical and photochemical properties of highly soluble phthalocyanines substituted with four 3,5-dimethylpyrazole-1- methoxy groups. Journal of Organometallic Chemistry 2011: 696; 3807-3815. doi: 10.1016/j.jorganchem.2011.09.002

17. Li M, Tian R, Fan J, Du J, Long S et al. A lysosome-targeted BODIPY as potential NIR photosensitizer for photodynamic therapy. Dyes and Pigments 2017; 147: 99-105. Doi: 10.1016/j.dyepig.2017.07.048

18. Lee SK, Tan KW, Ng SW. Topoisomerase I inhibition and DNA cleavage by zinc, copper, and nickel derivatives of 2-[2-bromoethyliminomethyl]-4-[ethoxymethyl]phenol complexes exhibiting anti-proliferation and anti-metastasis activity. Journal of Inorganic Biochemistry 2016; 159: 14-21. doi: 10.1016/j.jinorgbio.2016.02.010

19. Neves AP, Pereira MX, Peterson EJ, Kipping R, Vargas MD et al. Exploring the DNA binding/cleavage, cellular accumulation and topoisomerase inhibition of 2-hydroxy-3-(aminomethyl)-1,4-naphthoquinone Mannich bases and their platinum(II) complexes. Journal of Inorganic Biochemistry 2013; 119: 54-64. doi: 10.1016/j.jinorgbio.2012.10.007

20. Sinha P, Kumari N, Singh K, Singh K, Mishra L. Homoleptic bisterpyridyl complexes: synthesis, characterization, DNA binding, DNA cleavage and topoisomerase II inhibition activity. Inorganica Chimica Acta 2015; 432: 71-80. doi: 10.1016/j.ica.2015.03.026

21. Tabassum S, Zaki M, Afzal M, Arjmand F. Synthesis and characterization of Cu(II)-based anticancer chemotherapeutic agent targeting topoisomerase Iα:invitroDNA binding, pBR322 cleavage, molecular docking studies and cytotoxicity against human cancer cell lines. European Journal of Medicinal Chemistry 2014; 74: 509-523. doi: 10.1016/j.ejmech.2013.12.046

22. Liang X, Wu Q, Luan S, Yin Z, He C et al. W. A comprehensive review of topoisomerase inhibitors as anticancer agents in the past decade. European Journal of Medicinal Chemistry 2019; 171: 129-168. doi: 10.1016/j.ejmech.2019.03.034

23. Weijer R, Broekgaarden M, Krekorian M, Alles LK, van Wijk AC et al. Inhibition of hypoxia inducible factor 1 and topoisomerase with acriflavine sensitizes perihilar cholangiocarcinomas to photodynamic therapy. Oncotarget 2016; 7 (3): 3341-3356. doi: 10.18632/oncotarget.6490

24. Barut B, Sofuoğlu A, Biyiklioglu Z, Özel A. The water soluble peripherally tetra-substituted zinc(II), manganese(III) and copper(II) phthalocyanines as new potential anticancer agents. Dalton Transactions 2016; 45: 14301-14310. doi: 10.1039/C6DT02720B

25. Özel A, Barut B, Demirbaş Ü, Biyiklioglu Z. Investigation of DNA binding, DNA photocleavage, topoisomerase I inhibition and antioxidant activities of water soluble titanium(IV) phthalocyanine compounds. Journal of Photochemistry and Photobiology B: Biology 2016; 157: 32-38. doi: 10.1016/j.jphotobiol.2016.02.005

26. Demirbaş Ü, Göl C, Barut B, Bayrak R, Durmuş M et al. Peripherally and non-peripherally tetra-benzothiazole substituted metal-free, zinc(II) and lead(II) phthalocyanines: synthesis, characterization, and investigation of photophysical and photochemical properties. Journal of Molecular Structure 2017; 1130: 677-687. doi: 10.1016/j.molstruc.2016.11.017

27. Demirbaş Ü, Akyüz D, Barut B, Bayrak R, Koca A et al. Electrochemical and spectroelectrochemical properties of thiadiazole substituted metallo-phthalocyanines. Spectrochimica Acta Part A: Molecular and Biomolecular Spectroscopy 2016; 153: 71-78. doi: 10.1016/j.saa.2015.07.105

28. Demirbaş Ü, Pişkin M, Barut B, Bayrak R, Durmuş M et al. Metal-free, zinc(II) and lead(II) phthalocyanines functioning with 3- (2H-benzo[d][1,2,3]triazol-2-yl)-4-hydroxyphenethyl methacrylate groups: synthesis and investigation of photophysical and photochemical properties. Synthetic Metals 2016; 220: 276-285. doi: 10.1016/j.synthmet.2016.06.026

29. Demirbaş Ü, Pişkin M, Akçay HT, Barut B, Durmuş M et al. Synthesis, characterisation, photophysical and photochemical properties of free-base tetra-(5-chloro-2-(2,4-dichlorophenoxy) phenoxy)phthalocyanine and respective zinc(II) and lead(II) complexes. Synthetic Metals 2017; 223: 166-171. doi: 10.1016/j.synthmet.2016.12.004

30. Barut B, Demirbaş Ü, Özel A, Kantekin H. Novel water soluble morpholine substituted Zn(II) phthalocyanine: synthesis, characterization, DNA/BSA binding, DNA photocleavage and topoisomerase I inhibition. International Journal of Biological Macromolecules 2017; 105: 499-508. doi: 10.1016/j.ijbiomac.2017.07.072

31. Arslantaş A, Ağırtaş MS. The interaction between a zinc(II) phthalocyanine compound bearing octakis phenoxyacetamide substituents and calf thymus DNA. Turkish Journal of Chemistry 2018; 42: 1310-1320. doi: 10.3906/kim-1805-18

32. Kocak A, Yılmaz H, Faiz O, Andaç O. Experimental and theoretical studies on Cu(II) complex of N,N′-disalicylidene-2,3-diaminopyridine ligand reveal indirect evidence for DNA intercalation. Polyhedron 2016; 104: 106-115. doi: 10.1016/j.poly.2015.11.037

33. Fu XB, Zhang JJ, Liu DD, Gan Q, Gao HW et al. Cu (II)-dipeptide complexes of 2-(4'-thiazoly)benzimidazole: Synthesis, DNA oxidative damage, antioxidant and in vitro antitumor activity. Journal of Inorganic Biochemistry 2015; 143: 77-87. doi: 10.1016/j.jinorgbio.2014.12.006

34. Thamilarasan V, Jayamani A, Sengottuvelan N. Synthesis, molecular structure, biological properties and molecular docking studies on MnII, CoII and ZnII complexes containing bipyridine–azide ligands. European Journal of Medicinal Chemistry 2015; 89: 266–278. doi: 10.1016/j.ejmech.2014.09.073

35. Yıldız Ö, Çolak AT, Yılmaz M, İça T, Oztopcu-Vatan P et al. The syntheses, characterization, antimicrobial, DNA cleavage and cytotoxic activities of novel terephthalato complexes. Journal of Molecular Structure 2017; 1127: 668-674. doi: 10.1016/j.molstruc.2016.08.018

Supplementary information

1. Materials and equipment

All reactions were performed under an inert nitrogen atmosphere. 1-Phenoxy-2-propanol (**1**), 4-nitrophthalonitrile (**2**), 1,8-diazabicyclo[4.5.0]undec-7-ene, 1,3-diphenylisobenzofuran (DPBF), calf thymus-DNA (ct-DNA), ethidium bromide (EB), agarose, acetic acid, ethylenediaminetetraacetate (EDTA), β-mercaptoethanol (ME), bromophenol blue, xylene cyanol, glycerol, hydrogen peroxide (H_2O_2), potassium acetate, Tris-acetate, magnesium acetate, bovine serum albumin (BSA), and sodium dodecyl sulfate (SDS) were obtained from Sigma-Aldrich. Supercoiled pBR322 plasmid DNA was obtained from Thermo Scientific (SD0041). *E. coli* topoisomerase I enzyme was purchased from NEB (M0301L). All chemicals and reagents used were of analytical grade or higher.

^{1}H NMR spectra were recorded on a Varian XL-400 NMR spectrometer and chemical shifts were reported (δ) relative to Me_4Si (tetramethylsilane) as an internal standard. IR spectra were recorded on a PerkinElmer Spectrum One FT-IR spectrometer. The MS spectra were measured with a BRUKER Microflex LT by MALDI-TOF (matrix-assisted laser desorption ionization-time of flight) mass spectrometer technique using 2,5-dihydroxybenzoic acid (DHB) as a matrix. Methanol and chloroform were used as solvents in mass analysis and all mass analyses were conducted in positive ion mode. Melting points were measured by an electrothermal apparatus. The UV-Vis absorption spectra were recorded on a PerkinElmer Lambda 25 UV-Vis spectrophotometer at room temperature. The DNA cleavage and topoisomerase experiments were photographed using the Bio-Rad Gel Doc XR system and the results were calculated by the Image Lab Version 4.0.1 software program. The power density was measured using a power meter (Ophir sensor Nova II).

2. Synthesis

2.1. 4-(1-Phenoxypropan-2-yloxy)phthalonitrile (3)

1-Phenoxy-2-propanol (**1**) (3.00 g, 19.71 mmol) and 4-nitrophthalonitrile (**2**) (3.41 g, 19.71 mmol) were dissolved in dried DMF (20 mL). Anhydrous K_2CO_3 (4.08 g, 29.57 mmol) was added within 2 h to the reaction mixture. The mixture was stirred at 50 °C for 4 days and then it was poured into 250 mL of ice water, stirred for 1 h at room temperature, and filtered

off. The product was crystallized from ethanol. Yield 2.63 g (48%), mp 230–232 °C, $C_{17}H_{14}N_2O_2$. IR υ_{max}/cm^{-1}: 3078, 2985, 2937, 2229 (C≡N), 1590, 1489, 1321, 1239, 1172, 1054, 971, 847, 759, 692. ^{1}H NMR ($CDCl_3$) (δ: ppm): 7.710 (d, 1H, aromatic proton), 7.42–7.24 (m, 3H, aromatic protons), 7.098–6.870 (m, 4H, aromatic protons), 4.907, (m, H, -CH, aliphatic proton), 4.170 (m, 2H, -CH_2, aliphatic protons), 1.487 (d, 3H, -CH_3, aliphatic protons). ^{13}C NMR ($CDCl_3$) (δ: ppm): 161.774, 158.034, 135.199, 129.637, 129.527, 121.523, 120.347, 119.533, 116.024, 115.698 (C≡N), 115.276 (C≡N), 114.516, 114,446, 107.255, 74.025 (-CH), 70.751 (-CH_2), 16.683 (-CH_3). MALDI-TOF-MS (m/z): Calculated: 278.11; Found: 279.106 $[M+H]^+$.

2.2. Peripherally tetra-substituted zinc(II) phthalocyanine (4)

A mixture of phthalonitrile compound **3** (0.6 g, 2.16 mmol), n-pentanol (10 mL), 1,8-diazabicyclo[4.5.0]undec-7-ene (DBU) (5 drops), and equivalent amounts of anhydrous $Zn(CH_3COOH)_2$ was heated to 160 °C and stirred for 24 h at this temperature. After cooling at room temperature, the reaction mixture was precipitated by the addition of hexane and filtered off. After washing with ethyl acetate, acetone, and ethanol the solid product was purified with column chromatography using silica gel. Solvent system for column chromatography was chloroform:methanol (100:2). Yield: 330 mg (52%), mp >300 °C, $C_{68}H_{56}N_8O_8Zn$. IR (ATR) υ_{max}/cm^{-1}: 3059, 2973, 2928, 1598, 1486, 1393, 1336, 1223, 1116, 1086, 1044, 963, 880, 822, 744, 690. ^{1}H NMR (DMSO-d_6) (δ: ppm): 8.146–7.258 (bm, 32H, Ar-H, aromatic protons), 4.601 (bs, 4H, -CH, aliphatic protons), 4.161 (bs, 8H, -CH_2, aliphatic protons), 1.467 (bs, 12H, -CH_3, aliphatic protons). UV-Vis (DMF, 1×10^{-5} M): λ_{max}/nm (log ε): 679 (5.04), 611 (4.38), 353 (4.82). MALDI-TOF-MS, (m/z): Calculated: 1176.35, Found: 1177.056 $[M+H]^+$.

3. Singlet oxygen quantum yield (Φ_Δ)

Singlet oxygen quantum yield (Φ_Δ) determinations were carried out using the experimental set-up described in the literature [1]. Typically, 3 mL of the respective phthalocyanine (**4**) solutions (concentration = 1×10^{-5} M) containing the singlet oxygen quencher was irradiated in the Q band region with the photoirradiation set-up described in the literature [1]. The Φ_Δ value was determined in air using the relative method with Std-ZnPc (in DMSO) as a

standard. DPBF was used as a chemical quencher for singlet oxygen in DMSO. The Φ_Δ values of the studied phthalocyanine was calculated using Eq. 1:

$$\Phi_\Delta = \Phi_\Delta^{Std} \frac{R \cdot I_{abs}^{Std}}{R^{Std} \cdot I_{abs}} \quad , \qquad (1)$$

where Φ_Δ^{Std} is the singlet oxygen quantum yield for the standard. Std-ZnPc (Φ_Δ^{Std} = 0.67 in DMSO) [2] was used as standard. R and R_{Std} are the DPBF photobleaching rates in the presence of the compound **4** and the standard, respectively. I_{abs} and I_{abs}^{Std} are the rates of light absorption by compound **4** and the standard, respectively. I_{abs} was determined by using Eq. 2:

$$I_{abs} = \frac{\alpha.S.I}{N_A} \quad , \qquad (2)$$

To avoid chain reactions induced by DPBF in the presence of singlet oxygen [3], the concentration of quencher (DPBF) was lowered to ~3 × 10^{-5} M. Solutions of sensitizer (concentration = 1 × 10^{-5} M) containing DPBF were prepared in the dark and irradiated in the Q band region using the setup described in the literature [1]. DPBF degradation at 417 nm was monitored. The light intensity used for Φ_Δ determinations was found to be 6.60 × 10^{15} photons s^{-1} cm^{-2}.

4. DNA binding experiments

A solution of ct-DNA was prepared in 5 mM Tris-HCl and 50 mM NaCl (pH 7.2) followed by stirring for 3 days and kept at 4 °C for 1 week. In order to evaluate the percentage hypochromicity and intrinsic binding constant (K_b) of compound **4**, experiments were carried out using fixed concentrations of the compounds while varying the concentrations of ct-DNA. Increasing amounts of ct-DNA solution including the compounds were incubated for 10 min at room temperature and changes in the absorption spectra were monitored. EB was used as a positive control. The percentage of hypochromicity of compound **4** was calculated from Eq. 3:

$$Hypochromicity\ \% = \left(\frac{(\varepsilon f - \varepsilon b)}{\varepsilon f} \times 100\right). \quad (3)$$

The K_b of compound **4** was calculated using Eq. 4:

$$\frac{[DNA]}{(\varepsilon_a - \varepsilon_f)} = \frac{[DNA]}{(\varepsilon_b - \varepsilon_f)} + \frac{1}{K_b(\varepsilon_b - \varepsilon_f)}, \qquad (4)$$

where [DNA] is the concentration of ct-DNA. The apparent absorption coefficient ε_a = A_{obsd}/[compound], ε_f is the extinction coefficient of the free compound, and ε_b is the extinction coefficient of the compound when fully bound to DNA, respectively. In plots of [DNA]/(ε_a–ε_f) versus [DNA], K_b is given by the ratio of the slope to the intercept [4].

Competitive binding experiments of compound **4** with EB were performed using UV-Vis spectroscopy. The EB-(ct-DNA) complex was formed by adding EB:ct-DNA (75 μM : 75 μM) solution and gradually varying the concentrations of compound **4**, measured as the changes in the absorption spectra in the range of 425–550 nm [5].

5. DNA cleavage experiments

DNA cleavage properties of the compound were monitored by agarose gel electrophoresis using supercoiled pBR322 plasmid DNA without/with irradiation. The DNA-photocleavage studies were performed under light irradiation using light (white, 17.5 mW/cm^2, 10 min). Briefly, supercoiled pBR322 plasmid DNA was treated with increasing concentrations of compound **4** (6.25–50 μM) in buffer containing 50 mM Tris-HCl (pH 7.0). All samples were incubated at 37 °C for 1 h. Then loading buffer (bromophenol blue, xylene cyanol, glycerol, EDTA, SDS) was added and the mixtures were loaded onto 0.8% agarose gel with EB staining in TAE buffer (Tris-acetic acid-EDTA). Electrophoresis was carried out at 100 V for 90 min and the results were visualized by the Bio-Rad Gel Doc XR system and analyzed using Image Lab Version 4.0.1 [6].

To determine cleavage effects of compounds with oxidative agents, supercoiled pBR322 plasmid DNA and the compound were treated by adding oxidative agents such as hydrogen peroxide (H_2O_2), ascorbic acid (AA), and 2-mercaptoethanol (ME) without or with irradiation and analyzed according to the procedure described above [6].

6. *E. coli* topoisomerase I inhibition assay

E. coli topoisomerase I assays were carried out as described previously with modifications [7]. Camptothecin was used as a positive control. A mixture containing supercoiled pBR322 plasmid DNA and 2 units of *E. coli* topoisomerase I was incubated with/without compound **4** at 37 °C for 1 h in buffer including 50 mM potassium acetate, 20 mM Tris-acetate, 10 mM magnesium acetate, and 100 μg/mL BSA (pH 7.9 at 25 °C). Then

loading buffer was added to the reaction mixture. These reaction mixtures were loaded onto 0.8% agarose gel with EB staining in TAE and electrophoresed at 45 V for 3 h, and the image was photographed using the Bio-Rad Gel Doc XR system and calculated using Image Lab Version 4.0.1.

References

1. Durmuş M. Photochemical and photophysical characterization. In: Nyokong T, Ahsen V (editors). Photosensitizers in Medicine, Environment, and Security. New York, NY, USA: Springer, 2012, p. 141.

2. Akçay HT, Pişkin M, Demirbaş Ü, Bayrak R, Durmuş M et al. Novel triazole bearing zinc(II) and magnesium(II) metallophthalocyanines: synthesis, characterization, photophysical and photochemical properties. Russian Journal of Organometallic Chemistry 2013; 745-746: 133-140. doi: 10.1016/j.jorganchem.2013.08.029

3. Spiller W, Kliesch H, Wohrle D, Hackbarth S, Roder B et al. Singlet oxygen quantum yields of different photosensitizers in polar solvents and micellar solutions. Journal of Porphyrins and Phthalocyanines 1998; 2: 145-158. doi: 10.1002/(SICI)1099-1409(199803/04)2:2<145::AID-JPP60>3.0.CO;2-2

4. Bıyıklıoğlu Z, Barut B, Özel A. Synthesis, DNA/BSA binding and DNA photocleavage properties of water soluble BODIPY dyes. Dyes and Pigments 2018; 148: 417-428. doi: 10.1016/j.dyepig.2017.09.051

5. Kocak A, Yilmaz H, Faiz O, Andaç O. Experimental and theoretical studies on Cu(II) complex of N,N '-disalicylidene-2,3-diaminopyridine ligand reveal indirect evidence for DNA intercalation. Polyhedron 2016; 104: 106-115. doi: 10.1016/j.poly.2015.11.037

6. Fu XB, Zhang JJ, Liu DD, Gan Q, Gao HW et al. Cu (II)-dipeptide complexes of 2-(4'-thiazoly)benzimidazole: synthesis, DNA oxidative damage, antioxidant and in vitro antitumor activity. Journal of Inorganic Biochemistry 2015; 143: 77-87. doi: 10.1016/j.jinorgbio.2014.12.006

7. Yu X, Zhang M, Annamalai T, Bansod P, Narula G et al. Synthesis, evaluation, and CoMFA study of fluoroquinophenoxazine derivatives as bacterial topoisomerase IA inhibitors. European Journal of Medicinal Chemistry 2017; 125: 515-527. doi: 10.1016/j.ejmech.2016.09.053